An accurate and efficient Lagrangian sub-grid model

Document Version:
Publisher's PDF, also known as Version of Record (includes final page, issue and volume numbers)

Please check the document version of this publication:

• A submitted manuscript is the version of the article upon submission and before peer-review. There can be important differences between the submitted version and the official published version of record. People interested in the research are advised to contact the author for the final version of the publication, or visit the DOI to the publisher's website.
• The final author version and the galley proof are versions of the publication after peer review.
• The final published version features the final layout of the paper including the volume, issue and page numbers.

Link to publication

An accurate and efficient Lagrangian sub-grid model

Irene M. Mazzitelli,[1] Federico Toschi,[2] and Alessandra S. Lanotte[3,a)]

[1]*Dip. Ingegneria dell'Innovazione, Univ. Salento, 73100 Lecce, Italy and CNR-ISAC,
Via Fosso del Cavaliere 100, 00133 Roma, Italy*
[2]*Department of Applied Physics and Department of Mathematics and Computer Science,
Eindhoven University of Technology, Eindhoven 5600 MB, The Netherlands and CNR-IAC,
Via dei Taurini 19, 00185 Rome, Italy*
[3]*CNR ISAC and INFN, Sez. di Lecce, Str. Prov. Lecce Monteroni, 73100 Lecce, Italy*

A computationally efficient model is introduced to account for the sub-grid scale velocities of tracer particles dispersed in statistically homogeneous and isotropic, incompressible turbulent flows. The model embeds the multi-scale nature of turbulent temporal and spatial correlations, that are essential to reproduce multi-particle dispersion. It is capable to describe the Lagrangian diffusion and dispersion of temporally and spatially correlated clouds of particles. Although the model neglects intermittent corrections, we show that pair and tetrad dispersion results nicely compare with Direct Numerical Simulations of statistically isotropic and homogeneous 3D turbulence. This is in agreement with recent observations that deviations from self-similar pair dispersion statistics are rare events. © *2014 AIP Publishing LLC.* [http://dx.doi.org/10.1063/1.4894149]

I. INTRODUCTION

The transport of particles in turbulent flows is strongly sensitive to the multi-scale and multi-time fluctuations of the turbulent Eulerian velocity. For this reason, the dispersion of particles poses extraordinary challenges when the complexity of the flow geometry or the large Reynolds numbers requires the use of turbulence models. In particular, the modelisation of the small Eulerian scales can significantly alter the dynamics of particle dispersion. Particle dispersion in incompressible turbulence, either from extended or from localized sources,[1,2] is a very common phenomenon of practical importance for atmospherical, as well as for many applied problems.[3] Among the many possible examples, we remind here the dynamics and the spatial distribution of pollutants and pollen in the atmosphere[4–7] or oceanic flows,[8,9] the formation and the dynamics of small rain droplets in clouds,[10] the dynamics of colloidal aggregates in turbulence,[11,12] the combustion of fuel droplets, and the formation of soot particles in engines.[13]

The development of turbulence models and closures, to describe the effect of the *unresolved* or sub-grid scale (SGS) features of the Eulerian vector or scalar fields, has a long history dating back to Lilly and Smagorinsky (see Ref. 14). It is fair to say that nowadays there are a number of well-established *classical* SGS models for homogeneous and isotropic turbulence (HIT), adapted and extensively tested under a variety of conditions,[15] as well as more recent proposals keeping into account the phenomenology of turbulence beyond HIT (see e.g., Refs. 16 and 17).

The development of sub-grid models for Lagrangian turbulence has a relatively shorter history, partly due to the lack of accurate experimental and direct numerical simulation measurements of Lagrangian statistics in high Reynolds number flows. The recent availability of a large amount of Lagrangian statistics measurements in HIT[18–25] has allowed to quantitatively establish the phenomenological picture for tracers (reviewed in Refs. 26–28), and partially also for inertial point-particles.[29]

---

a)Author to whom correspondence should be addressed. Electronic mail: a.lanotte@isac.cnr.it

    26, 095101-1

The knowledge borrowed from experiments and direct numerical simulations has then promoted new research on Lagrangian sub-grid scale models for tracers, and inertial particles also (see e.g., Refs. 6, 30, and 31). The effects of small-scale temporal and spatial correlations on the dynamics of particles are an important problem.[32] In particular beyond *classical* measurements of the Lagrangian dynamics of a single particle and of particle pairs, the geometric features of multiparticles dispersion has also been investigated.[33–36]

Within the complex picture of Lagrangian dynamics, one of the most important point is that Lagrangian turbulence is more intermittent than Eulerian turbulence[37] and, as a result, one may have to pay additional care when using Gaussian models to model the Lagrangian velocity fields. Moreover, in HIT, the relative dispersion of tracers is mainly dominated by small-scale fluid motions: if these are neglected, particle pairs disperse at a much slower rate than the actual one (ballistic vs Richardson dispersion).

Traditionally, Lagrangian SGS motions are described by means of stochastic models. These are based on stochastic differential equations for the evolution of the velocity, assumed to be Markovian, along a particle trajectory. Stochastic models can be built up for single particle trajectories,[38] two-particle[39–41] and four-particle dispersion.[42,43] The literature on the topic is vast and we cannot review it here. What is important for the present discussion is that stochastic models for two-particle dispersion are generally inconsistent with single particle statistics, so that depending on the problem at hand one has to change model.

A different approach was developed in Lacorata *et al.*,[6] where a multiscale kinematic velocity field was introduced to model turbulent relative dispersion at sub-grid scales. The authors exploited Lagrangian chaotic mixing generated by a nonlinear deterministic function, periodic in space and time. This approach differs from kinematic models (e.g., Refs. 44 and 45), as it reproduces the effect of large-scale sweeping on particle trajectories.[46–48]

In the context of wall-bounded flows, Lagrangian SGS schemes have been proposed in terms of approximate deconvolution models based on the Eulerian field (see, e.g., Ref. 49), or in terms of force-based models.[50] Observables capable to discriminate between model error and drift induced errors were proposed.[51]

Most of these models rely on the knowledge of the resolved Eulerian velocity field. However, we note that models have been proposed to solve the Lagrangian dynamics self-consistently without an underlying Eulerian velocity field. This is for example the idea behind Smoothed Particle Hydrodynamics (SPH), i.e., a purely Lagrangian scheme to solve the Navier-Stokes equation, recently reviewed in Ref. 52. In Smoothed Particle Hydrodynamics, instead of solving the fluid equations on a grid, a set of particles are used , whose equations of motion are determined from the continuum Navier-Stokes equations.

An important issue concerns the possibility to build up models accounting for multi-particle dispersion, $\mathcal{N} > 2$, going beyond the pair separation dynamics. Multi-particle Lagrangian models invariably need to incorporate a mechanism correlating the sub-grid-scale velocities of the particles. Different approaches are possible. In Sawford *et al.*,[53] a two-particle stochastic model for 3D Gaussian turbulence[40,54] has been generalised to the problem of $\mathcal{N}$ tracers: these are constrained by pair-wise spatial correlations, implying that multi-point correlations are neglected. Interestingly, the model shows a good agreement of multi-point statistics with direct numerical simulations results. Alternatively, Burgener *et al.*[55] proposed to build spatial correlations between the fluid particles by minimising a Heisenberg-like Hamiltonian. In the Hamiltonian, the two-object coupling function is distance-dependent and with a power law behaviour. Ballistic separation and Taylor diffusion regimes in pair dispersion are clearly observed, while turbulent inertial-range dispersion *á la* Richardson is observed in specific conditions, only.

In this paper, we introduce a novel, accurate, and computationally efficient Lagrangian Sub-Grid Scale model (LSGS) for the dispersion of an arbitrary number of tracers in 3D statistically homogeneous and isotropic turbulent flows. The model is purely Lagrangian and it defines and evolves the velocities of tracers at their positions. The trajectories of $\mathcal{N}$ particles are simply obtained by time-integrating the Lagrangian velocities. It is primarily meant to reproduce Lagrangian dispersion at sub-grid scales, but it may be used as well as a rudimentary Lagrangian Navier-Stokes solver, much in the spirit of SPH.

The model encodes velocity fluctuations that scale in space and in time consistently with Kolmogorov's 1941 theory,[56] hence without intermittentcy corrections, and is self-consistent for an arbitrary number or density of tracers. An essential prescription for the model is the capability to correctly reproduce single-particle absolute diffusion together with multi-particle dispersion. For the latter, we require proper reproduction of inertial range pair dispersion (Richardson dispersion[25,27,28]), as well as the dynamics and the deformation of tetrads.

In a nutshell, the idea of the LSGS model is to define a multiscale relative velocity difference between two tracers, consistent with Kolmogorov inertial range scaling. Such velocity difference, characterized by the proper eddy turnover time, is able to reproduce Richardson dispersion for a single pair of tracers. The model is built up in a similar spirit of what done in Ref. 6 for tracer pair dispersion, but it is capable of ensuring consistent correlations between an arbitrary number of tracers according to their positions and relative distances. By accounting for spatial correlations among nearby tracers, we ensure that tracers close in space will experience very similar SGS velocities.

Beyond pair dispersion, we quantitatively validate the temporal evolution and dispersion properties of groups of four particles (tetrads), against Direct Numerical Simulations results.[34] An important property of any Lagrangian model for incompressible turbulence is the maintenance of a uniform spatial distribution of tracer particles. This issue is related to the incompressibility of the modeled velocity field. We investigate this issue at length in the Appendix. Our conclusion is that the degree of homogeneity can be kept controlled, and that possible small deviations from uniformity become negligible when the model is used as a SGS model in large-eddy simulations or any other large-scale numerical model.

The paper is organised as follows. In Sec. II, we introduce the LSGS model for an arbitrary number of tracers, and with an arbitrary large inertial range of scales. In Sec. III, we specify the model parameters and discuss the results for absolute, pair, and tetrad dispersion. Section IV is devoted to the concluding remarks.

II. THE LAGRANGIAN PARTICLE MODEL

In large-eddy simulations, the full tracer velocity is defined as the sum of the resolved Lagrangian velocity component, $V_i(x_i, t)$, and the sub-grid-scale contribution, $v_i(x_i(t), t)$. The larger scale components of the velocity, characterized by larger correlation times, sweep the smaller ones thus advecting both particles and small-scale eddies. This is a crucial feature of Lagrangian turbulence, sometimes neglected in synthetic models of Eulerian turbulence, that incorrectly describe pair dispersion.[46–48]

The Lagrangian sub-grid-scale model describes the 3D velocity, $v_i(x_i(t), t)$, at the position, $x_i(t)$, of the ith of the $\mathcal{N}$ tracer particles. The velocity fluctuations along each particle trajectory are the superposition of different contributions from eddies of different sizes. These eddies constitute a turbulent field, decomposed for convenience in terms of logarithmically spaced shells.

We consider the velocity of a tracer built as the sum of a set of fluctuations, u_n, of index n associated to a equispaced set of lengthscales, l_n. Given the largest length scale of the flow, L_0, smaller scales are defined as

$$l_n = \frac{L_0}{\lambda^n}, \qquad n = 0, \ldots, N_m - 1, \tag{1}$$

where N_m is the total number of modes, scales are logarithmically equispaced and the factor $\lambda > 1$ is conventionally chosen as $\lambda = 2^{1/4}$. Length-scales correspond to wave-numbers $k_n = 2\pi/l_n$, so that the velocity amplitudes and the associated turn-over times are defined as

$$u_n = q_0 \, k_n^{-1/3}, \qquad \tau_n = l_n/u_n, \tag{2}$$

where $q_0 = u_0 \, k_0^{1/3}$ is associated with the amplitude of the large-scale velocity.

A. Implementation of the LSGS

With the aim of making the description as clear as possible, we consider that the model is best illustrated by the following two-steps procedure:

Step 1: At time t, the positions $\mathbf{x}_i(t)$ of all $\mathcal{N}$ particles are given. The algorithm then generates— for each tracer i and for each lengthscale l_n—a *first* set of velocity vectors $\boldsymbol{\zeta}_n^{(i)}(t)$ (the three velocity components along the space directions x, y, z that are chosen independently from each other). Each of these velocities is the outcome of an Ornstein-Uhlenbeck (OU) process with correlation time $\tau_n = l_n/u_n$ and variance u_n^2, at the scale l_n. The time evolution of the OU process, for each spatial component of the velocity field of the ith particle at lengthscale l_n, is obtained according to[57]

$$\zeta_n^{(i)}(t + dt) = \zeta_n^{(i)}(t)\, e^{-dt/\tau_n} + u_n \sqrt{1 - e^{-2dt/\tau_n}}\,\beta\,, \tag{3}$$

where, for simplicity, we have omitted the sub-script for the spatial components. In (3), the variable β is a random number, normally distributed in the range $[0; 1]$. According to our definitions, each OU process is a normally distributed, random variable, $\zeta_n^{(i)}(t)$, whose mean value $\mu_n^{(i)}$ and standard deviation $\sigma_n^{(i)}$ are :

$$\mu_n^{(i)} = \zeta_{n_0} \exp\left[-(t - t_0)/\tau_n\right], \tag{4}$$

$$\sigma_n^{(i)} = u_n \sqrt{1 - \exp\left[-2(t - t_0)/\tau_n\right]}. \tag{5}$$

The equilibrium time $O(\tau_0)$ is needed for each mode to relax to a zero mean velocity and to the variance u_n^2. The velocity associated to the ith tracer particle is the superposition of N_m modes given by

$$\mathbf{v}^{(i)}(t) = \sum_{n=0}^{N_m-1} \boldsymbol{\zeta}_n^{(i)}(t)\,. \tag{6}$$

So doing, each particle has a multiscale, single-point velocity field which has the physical time correlations, but which does not respect space correlations yet. Indeed, based on the above algorithm, very different velocity fields could be assigned to particles residing in very close spatial position.

Step 2: In order to build up the proper spatial correlations and establish a correspondence between the modelled particle velocities and the two-point Eulerian statistics, we redefine for the ith particle the fluctuation associated to the nth mode as follows:

$$\mathbf{v}_n^{(i)}(t) = \sum_{j=1}^{\mathcal{N}} \boldsymbol{\zeta}_n^{(j)}(t) \cdot \left(1 - f_{l_n}(|\mathbf{x}_i - \mathbf{x}_j|)\right)\,. \tag{7}$$

Here the decorrelation function is such that $f(r) \propto r$ for $r \ll 1$ and $f(r) \simeq 1$ for $r \gg 1$. Its precise shape is not important and it may be as well a linear function, e.g.:

$$f(r) = |\mathbf{x}_i - \mathbf{x}_j|/l_n \quad \text{if} \quad |\mathbf{x}_i - \mathbf{x}_j| < l_n, \tag{8}$$

$$f(r) = 1 \qquad\qquad \text{if} \quad |\mathbf{x}_i - \mathbf{x}_j| \geq l_n. \tag{9}$$

Note that in (7), the nth mode velocity fluctuation for the ith particle is *determined* by the value of the nth mode velocity fluctuation of the particle j, with $j = 1, \ldots, \mathcal{N}$ spanning over the entire particle ensemble. Clearly, only particles closeby matter, while particles located very far from the ith particle will not matter.

The particle velocity resulting from the contributions of different eddies is then evaluated as

$$\mathbf{v}^{(i)}(t) = \sum_{n=0}^{N_m-1} \frac{1}{\mathcal{A}_n^{(i)}} \mathbf{v}_n^{(i)}(t). \tag{10}$$
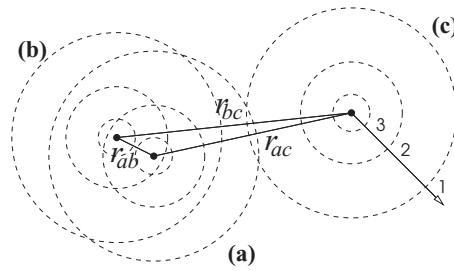
FIG. 1. A sketch of the model. The sketch is for the case of three particles (**a**, **b**, and **c**) with velocity fields composed by three eddies (1, 2, and 3, that corresponds to the three circles of diameter, respectively, l_1, l_2, and l_3). Tracers positions are indicated by black dots, while dashed circles are *correlation radii* relative to the eddies with diameter l_1, l_2, and l_3 (corresponding to shells 1, 2, and 3). The largest eddy described by the sub-grid-scale model may correspond to the smallest resolved eddy of the Eulerian Large-eddy simulation. In case of a purely Lagrangian evolution, i.e., without a large-scale model or a LES, the largest eddy corresponds to the integral scales of the system, L_0. The three modes of the velocity of particle "**a**" are computed by modulating the OU processes associated to particle "**a**"— $\zeta_i^{(\mathbf{a})}$ with $i = 1, 2, 3$ —and the OU processes attached to particles "**b**" and "**c**". This is done, in this simple example, according to: $\mathbf{v}_1^{(\mathbf{a})} = \zeta_1^{(\mathbf{a})} + \zeta_1^{(\mathbf{b})}(1 - \frac{r_{ab}}{l_1}) + \zeta_1^{(\mathbf{c})}(1 - \frac{r_{ac}}{l_1})$; $\mathbf{v}_2^{(\mathbf{a})} = \zeta_2^{(\mathbf{a})} + \zeta_2^{(\mathbf{b})}(1 - \frac{r_{ab}}{l_2})$; $\mathbf{v}_3^{(\mathbf{a})} = \zeta_3^{(\mathbf{a})}$, where we have kept into account the fact that (a) and (b) overlap with shells 1 and 2, while (a) and (c) overlap only with shell 1.

The normalization factor that preserves the variance is given by

$$\mathcal{A}_n^{(i)} = \sqrt{\sum_{j=1}^{\mathcal{N}} (1 - f_{l_n}(|\mathbf{x}_i - \mathbf{x}_j|))^2}. \tag{11}$$

As a result of this procedure, space correlations are introduced among the velocities of the whole particle ensemble. Particle velocities are no longer statistically independent, but behave as *responding* to the same local velocity fluctuations. In Figure 1, a graphic sketch of the model is given for the case of three Lagrangian tracers, with a few modes velocity field.

Note that, from (6), the variance of each velocity component along x, y, z is

$$\langle v'^{(i)}(t)^2 \rangle = \sum_{n=0}^{N_m - 1} \langle \zeta_n^{(i)}(t)^2 \rangle, \tag{12}$$

since modes are independent, $\langle \zeta_n^{(i)}(t) \zeta_{n'}^{(i)}(t) \rangle = 0$ for $n \neq n'$. If by physical arguments, we require a velocity field with root-mean-square values to be $v_{rms} = u_0$, it is enough to introduce in the velocity definition given in Eq. (6) or Eq. (10), the norm $\mathcal{F}$ defined as

$$\mathcal{F}^2 = \frac{u_0^2}{\sum_{n=0}^{N_m - 1} u_n^2}. \tag{13}$$

It is worth mentioning that the model has a tunable free parameter, corresponding to the turbulent energy dissipation rate $\epsilon \propto u_0^3 / L_0$. If used as a sub-grid, such parameter is provided by the large-scale model (e.g., a large-eddy simulation), and can then be used to fix the ratio among large-scale velocity and length values. In the absence of a large-scale model, an energy dissipation rate can be fixed up to constant $O(1)$.

We note that from a computational point of view, the simplest implementation of the LSGS model scales with the square of the number of particles that are simulated $\mathcal{N}^2$, but it can be easily optimized with standard Molecular Dynamics algorithms (e.g., by using a linked list).

To validate the model against observations for statistically homogeneous and isotropic 3D Lagrangian turbulence, we consider in the following the most challenging case corresponding to $V = 0$, when the sub-grid-scale model is solely responsible for the dynamics of tracers at all scales. Thus, to simplify the text, from now on the term "sub-grid" is dropped and we speak of tracers velocities; moreover, we adopt the shorthand notation $\boldsymbol{v}_i(t) \equiv \boldsymbol{v}_i(\boldsymbol{x}_i(t), t)$.
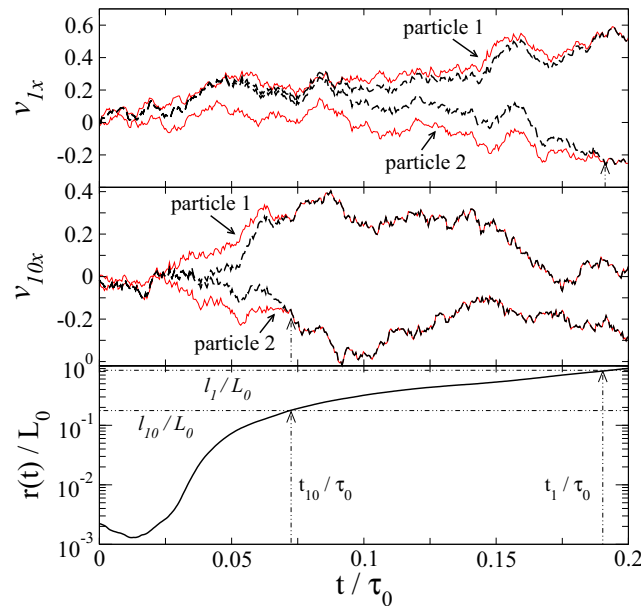
FIG. 2. Particle velocity modulation in the case of a single pair, initially placed at a separation distance r_0 smaller than the smallest eddy of the fluctuating velocity $r_0 < l_{N_m-1}$, with $N_m = 31$. Top: velocity fluctuation (x- component only) associated to the mode $n = 1$. Middle: the same but for the mode $n = 10$. In both cases, the curves represent: particle 1 OU process is the grey continuous line (red), particle 2 OU process is also plotted with a grey continuous line (red), particle 1 and 2 modulated velocity (black dashed lines). Bottom: the time evolution of the two particles separation $\mathbf{r}(t) = \mathbf{x}_1(t) - \mathbf{x}_2(t)$.

A first glance on the behaviour of the model can be appreciated in Figure 2. Here we consider the results of a simulation with only a pair of particles. The pair is initialised with relative separation r_0 smaller than the smallest eddy l_{N_m-1} of the velocity field. Simulation parameters are summarised in Table I, case $N_m = 31$. For plotting purpose, we selected two modes, namely, mode $n = 1$ of length scale $l_1 = L_0/\lambda$ and mode $n = 10$, with $l_{10} = L_0/(\lambda)^{10}$. The OU processes, $\zeta_{nx}^{(i)}(t)$ given by (3), resulting from the first step of the procedure are compared with their modulation due to nearby particle, see Eq. (7). In the beginning, when they are very close, the two tracers possess the same velocity (in the figure, the x component only is shown). When their separation becomes larger than the mode of length-scale l_n (in the example $n = 1$ and $n = 10$) particle velocities decorrelate, and thus each particle velocity collapses on its single-particle behaviour. As expected, decorrelation is faster for the $n = 10$ with respect to $n = 1$ mode, since for the former the eddy turnover time is smaller than for the latter.

Before discussing the performances of the model in the case of particle diffusion and dispersion, a more general remark is needed. As it is well known, the satisfaction of the fluid governing equation yields constraints on the particle system. For instance, the continuity equation $\nabla \cdot \mathbf{u}(\mathbf{x}, t) = 0$ is satisfied when the particle density in space is uniform and constant at all points.[58] In stochastic approaches to Lagrangian particle velocity, physical information is used to constrain the form of the stochastic differential equation. The noise term has to be diffusive, while the drift term can be

TABLE I. Model parameters, the symbols indicate: q_0 entering the definition of the root-mean-square velocity u_0; N_m the total number of modes; L_0 and l_{N_m-1} the largest and smallest model length scales; and τ_0 and τ_{N_m-1} the largest and the smallest time scales. The ratio of the simulation time step dt to the fastest time scale τ_{N_m-1} is $dt/\tau_{N_m-1} \simeq 1/60$, in both cases.

N_m	q_0	L_0	l_{N_m-1}	τ_0	τ_{N_m-1}
31	0.4	10	5.5×10^{-2}	21	6.7×10^{-1}
62	0.4	10	2.6×10^{-4}	21	1.9×10^{-2}

specified on the basis of the Eulerian statistics of the flow. The physical request is that an initially uniform particle distribution will remain such, after Lagrangian evolution (from the Eulerian point of view, a well-mixed scalar field remains so). In 3D there is no unique form for the drift term, but there are a number of available solutions.[40,54]

Tracer uniform distribution is clearly a crucial feature for a SGS model for incompressible turbulence. In the Appendix, we discuss a series of tests we performed to assess the spatial distribution properties of the Lagrangian tracers, or in other words to assess the *incompressibility* of the particle velocity field.

III. RESULTS

We now discuss the results of two sets of numerical simulations, characterized by different values of the total number of modes N_m, at fixed values of the integral scale L_0 and root-mean-square velocity u_0. Increasing the number of modes at fixed L_0 and u_0 results in an extension of the inertial range of turbulence. For each set of numerical simulations, mean values are computed by ensemble averaging over 50 simulations, each containing 100 particle pairs. Particles are initially uniformly distributed in space, and such that the initial pair separation is smaller than the smallest eddy in the velocity, l_{N_m-1}. Their total number is $\mathcal{N} = 10^4$. The simulation parameters are reported in Table I.

We first consider the absolute dispersion, that is, the mean displacement of a single particle with respect to its initial position. The statistical behaviour is expected to be ballistic for correlated scales, followed by simple diffusion *à la* Taylor at scales larger than the velocity integral scale L_0. To this aim we compute:

$$D(t) = \langle [\mathbf{x}(t) - \mathbf{x}(0)]^2 \rangle, \tag{14}$$

where $\mathbf{x}(t)$ is the position at time t of a particle that was in $\mathbf{x}(0)$ at the initial time $t = 0$ and the brackets $\langle \cdot \rangle$ indicate ensemble average. From Figure 3, we observe that single particle diffusion is well represented by the model. At time scales of the inertial range, the slope is well approximated by the ballistic t^2 power law, whereas at large times, $t > \tau_0$, the diffusive scaling law sets in.

A. Tracer pair dispersion

The separation statistics of pairs of particles, labeled 1 and 2, is defined via the moments of the separation vector $\mathbf{r}(t) = \mathbf{x}_1(t) - \mathbf{x}_2(t)$. In statistically homogeneous and isotropic turbulence, the separation distance $r = |\mathbf{r}|$ is the key observable for the problem of relative dispersion.
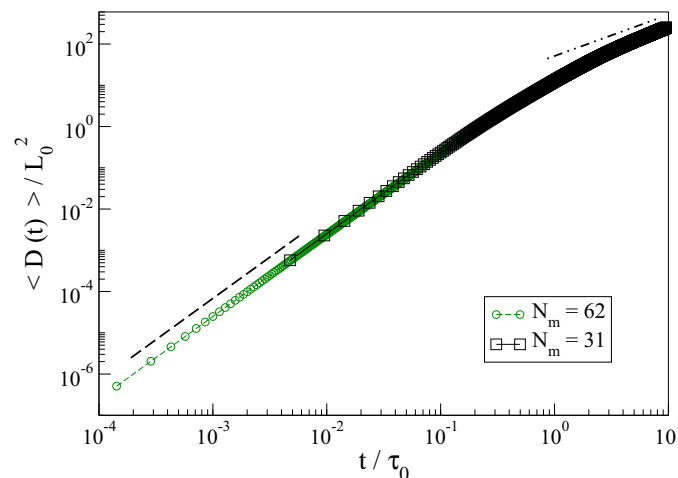

FIG. 3. Log-log plot of tracers absolute dispersion for the simulations with $N_m = 31$ (black squares) and $N_m = 62$ (green circles). Simulation with $N_m = 31$ modes was carried on for a longer time, whereas simulation with $N_m = 62$ extends to smaller times, owing to the smaller time step. The straight lines indicate, respectively, the t^2 ballistic behaviour (dashed line), and the diffusive t behaviour (dashed dotted line).
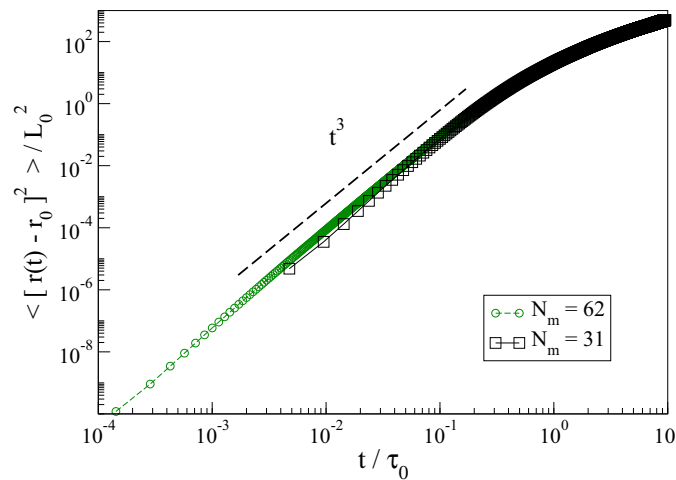
FIG. 4. Log-log plot of particle relative dispersion for the simulations with $N_m = 31$ (black squares) and $N_m = 62$ (green circles). The straight line indicates the Richardson t^3 scaling regime for the inertial range of scales.

We first report results on the statistics of

$$\langle [\mathbf{r}(t) - \mathbf{r}_0]^2 \rangle_{r_0} = \langle \{[\mathbf{x}_1(t) - \mathbf{x}_2(t)] - [\mathbf{x}_1(0) - \mathbf{x}_2(0)]\}^2 \rangle , \qquad (15)$$

to better highlight the scaling behaviours. Two regimes characterize the pair dispersion for inertial-range initial distances r_0,

$$\langle [\mathbf{r}(t) - \mathbf{r}_0]^2 \rangle_{r_0} \simeq t^2 S_2(r_0) , \qquad (16)$$

$$\langle \mathbf{r}(t)^2 \rangle \simeq g\, t^3 . \qquad (17)$$

The first behaviour is the so-called Batchelor regime[27] due to the memory of the initial velocity difference. In Eq. (16), $S_2(r)$ is the Eulerian second-order structure function at scale r. The Batchelor scaling occurs on time scales of the order of the eddy-correlation time at scale r_0. The second is the Richardson regime, independent of the initial separation, taking place asymptotically on times scales much larger than the eddy-turnover time at scale r_0, and much smaller than the integral time scale. In Figure 4, we plot $\langle [\mathbf{r}(t) - \mathbf{r}_0]^2 \rangle$, where the average is taken over pairs whose initial separation r_0 is much smaller than the smallest scale l_{N_m-1}, accordingly the ballistic regime is very short, and the asymptotic Richardson regime is readily observed. Note that our model has the inertial range correlation of 3D turbulence built in, and thus cannot reproduce dissipative range behaviours where tracer pair dispersion is exponential and the rate of separation is given by the leading Lyapunov exponent.[25] However it is possible, when needed, to modify the model and include a viscous range of scales: a way to do it is to use a Fourier implementation of the so-called Batchelor-like parametrization of the fluid velocity.[59]

The existence of Richardson regime in 3D turbulence is often debated. In addition to the memory of the initial conditions, both experimental and numerical measurements have to deal with the limited extension of the inertial range, and with crossover regimes from the inertial scales toward the integral scale, and from the inertial scales toward the dissipative scale.

A better suited observable, allowing to partially overcome issues due to a limited inertial range, is obtained by using fixed-scale statistics.[60] It consists of fixing a set of thresholds, $r_n = \rho^n r_0$, with the factor $\rho > 1$ and $n = 1, 2, 3, ...$, and then calculating the time T it takes for the pair separation to change from r_n to r_{n+1}. If $\rho = 2$ such time is also called the *doubling time*. Here we compute the Finite-Size Lyapunov Exponent (FSLE) (Ref. 61), in terms of the mean time $\langle T_\rho(r) \rangle$ it takes for pair separation r to grow to ρr. In the present analysis, we used $\rho = 1.25$: note that the choice of $\rho > 1$ is irrelevant for the scaling properties, but only fixes the threshold spacing and enters in the mean
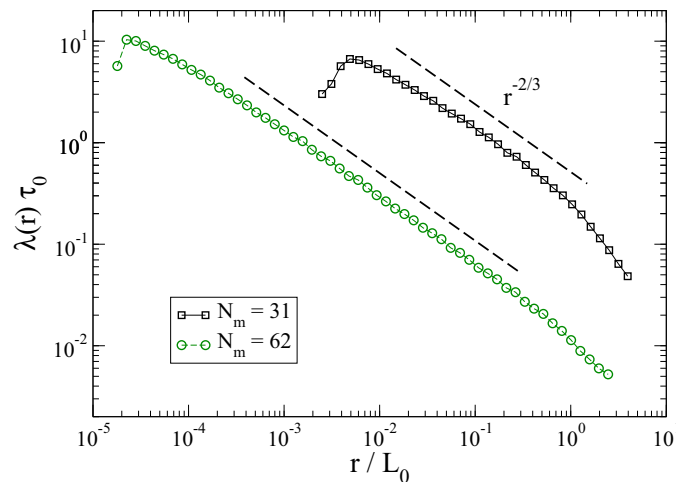
FIG. 5. Log-log plot of the Finite Size Lyapunov Exponent $\lambda(r)$ for the numerical simulations with $N_m = 31$ (black squares) and $N_m = 62$ (green circles). The straight dashed lines indicate the $r^{-2/3}$ scaling regime.

time expression as a prefactor.[25,62] The FSLE is defined as

$$\lambda(r_n) = \frac{\log \rho}{\langle T_\rho(r_n) \rangle} .\tag{18}$$

In the limit of an infinitesimal threshold r_n, the FSLE recovers the leading Lypanuov exponent of the turbulent flow.[61] In our model however there is no tangent space dynamics, and so the FSLE has a well defined meaning only in the inertial range of scales. By dimensional scaling arguments, if the mean separation grows as $\langle r(t)^2 \rangle \sim t^3$, then the FSLE behaves as $\lambda(r) \sim r^{-2/3}$. At scales larger than the integral scale L_0, we expect $\lambda(r) \sim r^{-2}$.

In Fig. 5, we plot the FSLE measurements for the two sets of numerical simulations performed. Since by construction all scales r, with $l_{N_m-1} < r < L_0$, belong to the inertial range, we observe the $\lambda(r) \sim r^{-2/3}$ scaling only. At large scales, we detect a steeper slope, associated to Taylor diffusion. Whereas at scales smaller than the smallest length-scale of the model, the FSLE drops due to a statistical effect.

B. Tetrad dispersion

The interest in studying the displacement statistics of a bunch of particles is that it can be used to describe moments of a passive scalar field, satisfying an advection-diffusion equation. This has been exploited in the past to assess the intermittent statistics of a passive scalar field advected by a synthetic Gaussian velocity field,[63] or by a 2D turbulent velocity field in the turbulent regime of inverse cascade of energy.[64] Unfortunately, similar results do not yet exist for 3D turbulence. On the other hand, Lagrangian multi-particle motion is very important when studying dispersion and mixing properties, both in ideal (i.e., statistically homogeneous and isotropic) and in real flows.

Beside pair dispersion, tetrad dispersion and its modelling have attracted much attention in the last years:[25,43,53,65] indeed, the time evolution of four tracers is the building block of a phenomenological model to describe the Lagrangian dynamics over a volume region with characteristic scales lying in the inertial range;[33] additionally, it is a better candidate than a tracer pair to describe geometrical properties in a turbulent flow, such as vortex stretching, and vorticity/strain alignment.

Within the proposed model, we have performed series of simulations with tracer particles initially arranged on regular tetrahedron of side $l_{N_m-1}/2$, so to have a narrow distributions for tetrads initial conditions. Moreover, the initial distribution of the tetrad centre of mass and orientation is random uniform in the computational domain. To achieve good statistics, we collected 50 simulations, each containing 100 tetrahedron. The model parameters are those listed in Table I, case $N_m = 62$.
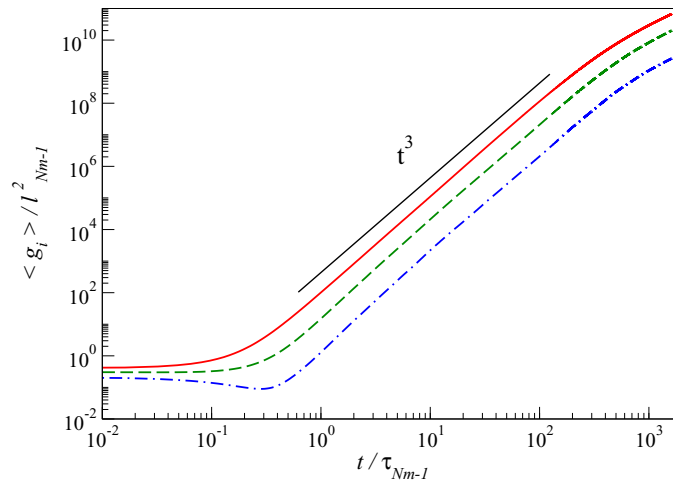
FIG. 6. Log-log plot of the mean eigenvalues of the inertia matrix, as a function of time. From top $\langle g_1 \rangle$, then $\langle g_2 \rangle$ and $\langle g_3 \rangle$. The straight line indicates the t^3 Richardson scaling law for the inertial range of scales.

The evolution of the tetrad shapes in a statistically homogeneous flow is conveniently analysed by performing a change of coordinate,[33] from the particle positions $\mathbf{x}_i$, $i = 1, 2, 3, 4$ to the reduced set of coordinates $\boldsymbol{\rho}_m$, $m = 0, 1, 2, 3$, defined as

$$\boldsymbol{\rho}_0 = \frac{1}{4} \sum_{i=1}^{4} \mathbf{x}_i \,, \tag{19}$$

$$\boldsymbol{\rho}_m = \frac{1}{\sqrt{m(m+1)}} \sum_{i=1}^{m} (\mathbf{x}_i - \mathbf{x}_{m+1}) \,. \tag{20}$$

While the centre of mass diffuses in the flow, the geometrical information is contained in the square symmetric inertia matrix $\mathbf{I} = \boldsymbol{\rho} \boldsymbol{\rho}^T$, with column vectors $\boldsymbol{\rho}_m$, $m = 1, 2, 3$. Owing to the homogeneity of the velocity field and of the initial tetrad distribution, the statistics does not depend on the centre of mass $\boldsymbol{\rho}_0$.
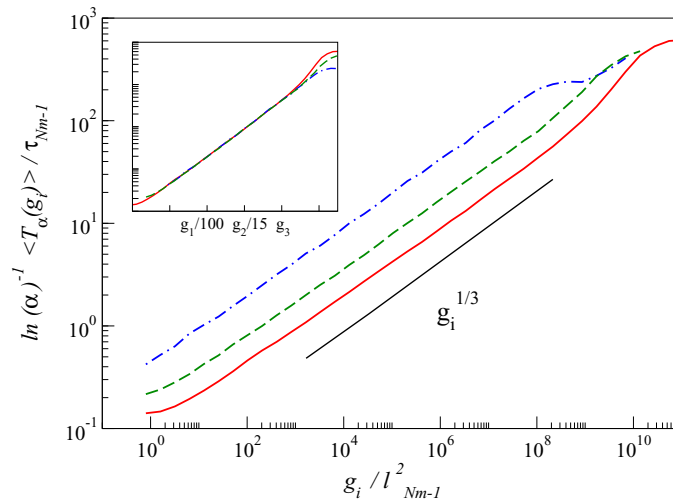

FIG. 7. Mean doubling-time values for the eigenvalues of the inertia matrix. From top $\langle T_\alpha(g_3) \rangle$, then $\langle T_\alpha(g_2) \rangle$ and $\langle T_\alpha(g_1) \rangle$, with $\alpha = 2$. In the inset the three curves are plotted, after rescaling g_1 and g_2 with the factors 100 and 15, respectively, to obtain an overlap.

The matrix admits real positive eigenvalues, g_i, that can be ordered according to: $g_1 \geq g_2 \geq g_3$. The tetrahedron dimension is given by $r = \sqrt{2/3\,tr(\mathbf{I})} = \sqrt{2/3(g_1 + g_2 + g_3)}$ and the volume is $V = 1/3\sqrt{det(\mathbf{I})} = 1/3\sqrt{g_1 g_2 g_3}$. It is convenient to introduce the adimensional quantities $I_i = g_i/r^2$ (where $I_1 + I_2 + I_3 = 1$), whose relative values give an indication of the tetrahedron shape. For a regular tetrahedron $I_1 = I_2 = I_3 = 1/3$; when the four points are coplanar $I_3 = 0$; when they are aligned $I_2 = I_3 = 0$.

We remark that by means of a stochastic model for tetrad dispersion, Devenish[43] recently obtained values for the I_i indices in agreement with those of Direct Numerical Simulations of 3D turbulence.

In Fig. 6, we present the temporal evolution of the mean eigenvalues of $\mathbf{I}$. Numerical results show good agreement with Richardson prediction, i.e., $\langle g_i \rangle \simeq t^3$. This issue is further verified by measuring fixed scale statistics. To this aim, we compute the average time $\langle T_\alpha(g_i) \rangle$ it takes for each eigenvalue g_i to increase its value of a factor α, with $\alpha = 2$. Hence we measure the average doubling times of the eigenvalues g_i, $\langle T_\alpha(g_i) \rangle$.

Results are plotted in Fig. 7. They indicate the existence of a wide inertial range, where the slope of the exit-time is $g_i^{1/3}$, matching Richardson prediction.[34] In addition, as shown in the inset,
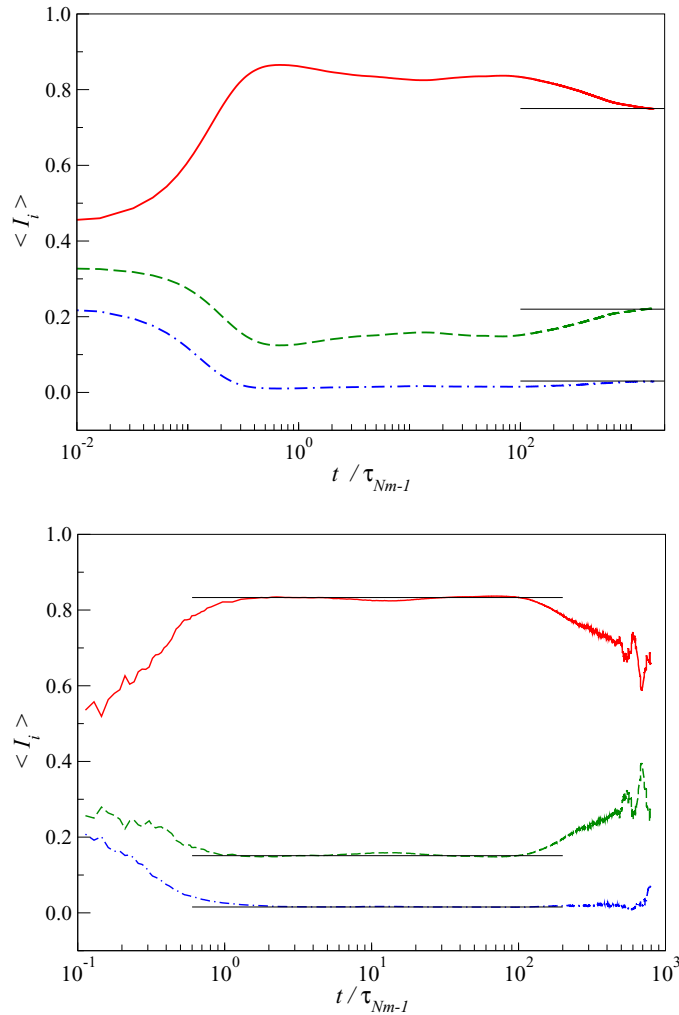

FIG. 8. Average shape parameters $\langle I_i \rangle$ as a function of time. On the left: average upon all tetrads. The straight lines indicate the asymptotic values for Gaussian distributed particles $I_1 = 0.75$, $I_2 = 0.22$, $I_3 = 0.03$. On the right: average upon tetrads whose g_i belongs to the inertial range. The straight lines are best fits for $1 < t/\tau_{Nm-1} < 100$: $I_1 = 0.833$, $I_2 = 0.151$, and $I_3 = 0.0155$.

the three eigenvalues overlap after rescaling g_1 and g_2 respectively with the factors 100 and 15. These scaling factors yield to $I_1 \simeq 0.862$, $I_2 \simeq 0.129$, $I_3 \simeq 0.0086$, i.e., on average very elongated tetrahedra prevail.

The existence of a range where, after rescaling on the horizontal axis, the values of the doubling-times are the same for the three eigenvalues implies that the tetrads increase their dimension while maintaining the same (elongated) shape. These results can be compared with the DNS of Ref. 34. They show qualitative agreement, though the values of the rescaling factors applied to achieve the exit-times collapse are different.

In Fig. 8 (left), we present the behaviour of the $\langle I_i \rangle$, with $i = 1, 2, 3$, as a function of time. The coefficients display, over a large time interval, values consistent with elongated tetrahedra. At large time lags, for $t/\tau_0 \sim 1$ (i.e., $t/\tau_{N_m-1} \sim O(10^3)$), they tend to the values obtained for tetrads formed from Gaussian distributed particles, as expected at scales larger than the correlation lengths of the velocity field.[65]

A further analysis can be done to better highlight the scaling properties of the tetrad separation process. In Fig. 8 (right), the $\langle I_i \rangle$ are computed selecting at each time step those tetrads whose mean doubling-time $\langle T_\alpha(g_i) \rangle$ follows the Richardson inertial range scaling. This corresponds to selecting tetrads whose eingenvalues are $1 < g_1/l_{Nm-1}, g_2/l_{Nm-1} < 10^9$, $1 < g_3/l_{Nm-1} < 10^8$. The figure shows the presence of a plateau where the values of the indexes are $\langle I_1 \rangle = 0.833 \pm 0.004$, $\langle I_2 \rangle = 0.151 \pm 0.003$, and $\langle I_3 \rangle = 0.0155 \pm 0.0007$. Again, there is some discrepancy with the direct numerical simulations results for HIT, where it was measured $\langle I_3 \rangle = 0.011 \pm 0.001$ and $\langle I_2 \rangle = 0.135 \pm 0.003$.[25] However, these values confirm the presence of elongated structures in the inertial range, with the index $\langle I_3 \rangle$ larger with respect to the expectation value for Gaussian distributed particles.

IV. CONCLUSION

A novel Lagrangian model is presented aimed at accurately reproducing the statistical behaviour of clouds of particles dispersed in incompressible, statistically homogeneous, and isotropic turbulent flows. The model reflects the multi-scale nature of the direct energy cascade of 3D turbulence. While the model is primarily meant to be used as a sub-grid model—it evolves fluid tracers sub-grid velocities that are correlated according to their relative distances—it may be adapted to solve the Navier-Stokes equations by a Lagrangian approach (in the spirit of smoothed-particle hydrodynamics solvers).

To assess the model performances and accuracy, we presented several validations based on comparison with recent investigations on the phenomenology of fluid tracers in high-resolution, high-statistics Direct Numerical Simulations. The first validation is based on the results of two simulations that differ only by total number of modes, while the large length- and velocity-scales are kept constant. We showed that the model can reproduce Richardson law for the pair dispersion statistics. It is important to stress that the width of the inertial range can be *a priori* fixed by tuning the sub-grid model parameters.

With respect to multi-particle statistics, we analysed the dispersion of tracers initially located on the side points of tetrahedra. Also in this case, we could observe a good agreement with results obtained in direct numerical simulations of homogeneous and isotropic turbulence.[34]

Two important approximations have been adopted to build up the model: velocity statistics are Gaussian and self-similar. Deviations from Gaussianity could be of interest if the tracer particle model is used to reproduce stationary statistics of turbulent velocity increments (e.g., the four-fifth law).[66] In the present formulation of the model, we neglected such feature and showed that this does not affect results for pair and tetrad dispersion.

Neglecting intermittency may also be a limitation since non-self-similar corrections to the Richardson's picture have been detected in the tails of pair separation distribution.[2, 23] Intermittency could be introduced by building up synthetic multi-affine processes.[3, 67] This is left for future investigations.

Based on the accuracy of the results, it appears that the potential of the model for practical use is high. First of all, it can be applied, within the restrictions discussed in the paper, to an arbitrary number of fluid tracers and the computational cost will grow with the number of tracers. Moreover

the model parameters can be chosen to achieve the desired extension of the inertial range. Finally, the absence of a grid makes the method suitable also for complex situations, for instance in the presence of free surfaces. The capabilities of the model in more complex flows, e.g., shear and channel flows, will be a matter of future investigations. Finally, the model may be easily modified to describe inertial heavy point-like particles.[68]

ACKNOWLEDGMENTS

APPENDIX: PARTICLE SPATIAL DISTRIBUTION

In order to test particle model incompressibility, we performed the following experiment. We seeded a periodic cubic domain with $\mathcal{N} = 1000$ particles, uniformly distributed. The particle velocity field has $N_m = 31$ velocity modes, that we followed for a few large eddy-turnover times, τ_0. An uniform distribution of $\mathcal{N}$ particles in the volume $\mathcal{V}$ means that, after coarse-graining the volume in cells of size R, the number of particles in each cell, dubbed $n(R)$, will be a random variable with Poisson distribution,

$$p_R(n) = \frac{(\lambda_R)^n}{n!} \exp(-\lambda_R). \tag{A1}$$

Here $\lambda_R = \mathcal{N}/(L/R)^3$ is the average number of particles in a cell of size R^3 and $\mathcal{V} = L^3$ is the total volume considered. From (A1), it is easy to derive

$$\langle n^2 \rangle = \langle n \rangle^2 + \langle n \rangle. \tag{A2}$$

Possible deviations from the uniform distribution can be systematically quantified, scale by scale, in terms of the coefficient:

$$\mu(R) = \frac{\sigma_R^2}{\lambda_R^2} = \frac{\langle n^2 \rangle - \langle n \rangle^2}{\langle n \rangle^2}, \tag{A3}$$

where for a uniform distribution $\langle n(R) \rangle = \lambda_R = \rho R^3$ and $\rho = \mathcal{N}/\mathcal{V}$ is the particle number density, thus $\mu(R) = 1/(\rho R^3)$. Deviation from such behaviour can be also quantified in terms of the two-points correlation in the particle distribution.

The test has been performed within three periodic boxes of sides, respectively, $2L_0$, $4L_0$, and $8L_0$, whose results are presented in Figure 9. The plots show that, on the small scales, uniformity is retained during the temporal evolution. However, on the large scales, spatial correlations may develop, being more intense when the box dimension is of the same order of the large-eddy scale, and decaying at increasing the ratio L/L_0. Therefore, for $L/L_0 \gg 1$, particle spread uniformly within the domain at all scales.

Note that, in order to take into account the effect of molecular diffusion on the smallest scales (i.e., scales smaller than l_{N_m-1}), a random fluctuation could be added to the velocity fields of coincident particles. In fact, according to our model, two or more particles, residing at the same location at the same time, will be subjected to the same velocity, so they will stick together for all subsequent times, while molecular diffusion would guarantee that coincident particles always separate, see Ref. 40. In practice, we found that it was not needed to include this random diffusion because these occurrences are very unlikely. This is confirmed by the behaviour of $\mu(R)$ on the very small scales.
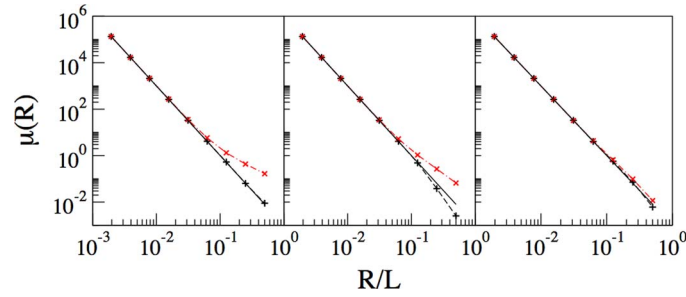
FIG. 9. Coefficient $\mu(R)$ as a function of R/L for simulation with $L = 2L_0$ (left), $L = 4L_0$ (centre), and $L = 8L_0$ (right). Results indicate: time $t = 0$ (black pluses), time $t = 2\tau_0$ (red crosses), and the uniform distribution expectation, $1/(\rho R^3)$ (black straight line).

Results of Fig. 9 have a clear interpretation: particles tend to spread uniformly, but the velocity modulation on the large scale induces spatial correlations. These can be further quantified and controlled according to the simple arguments that follows.

Starting from any initial spatial condition, when $t > \tau_0$ the average distance of one particle to its closest neighbour, d_1, can be estimated by the expression:[69]

$$d_1 = \frac{1}{\pi^{1/2}} \Big[\Gamma\Big(\frac{D}{2} + 1\Big) \Big]^{1/D} \Gamma\Big(1 + \frac{1}{D}\Big) \Big(\frac{\mathcal{V}}{\mathcal{N}}\Big)^{1/D}, \tag{A4}$$

where Γ is the Euler Gamma function, $D = 3$ the space dimension, $\mathcal{V}$ the volume, and $\mathcal{N}$ the total number of particles. Numerical results agree with the theoretical expectation for randomly distributed particles, Eq. (A4). The deviation of $\mu(R)$ from $1/(\rho R^3)$ occurs at a scale $R \sim d_1$ (i.e., R/L ~ 0.055 for $\mathcal{N} = 1000$), because mode velocities on all scales larger than d_1 are correlated. Clearly, the larger the number of correlated modes, the stronger the deviations from uniformity.

We remark that, when $L_0 = 10$ and $N_m = 31$, there are 13 modes with length scale larger than $d_1 = 1.1$ (average particle distance in simulations with $L = 2L_0$) and only 5 modes with length scale larger than $d_1 = 4.4$ (average distance when $L = 8L_0$). This explains the more intense deviations detected in the first plot of Figure 9 (first from the left), with respect to the third plot (third from the left).

In general, the number of correlated modes N_c depends on the integral scale L_0, on the model parameter λ, and on the particle density ρ, according to

$$N_c = int\left(1 + log_\lambda \frac{L_0}{d_1}\right), \tag{A5}$$

$$= int\left(1 + log_\lambda \left(\frac{\sqrt{\pi}\, L_0\, \rho^{1/3}}{\Gamma(5/2)^{1/3}\, \Gamma(4/3)}\right)\right). \tag{A6}$$

The average distance d_n of a particle to its nth neighbour can also be computed. Recalling that one point is the nth neighbor of another one if there are exactly $n - 1$ other points that are closer to the latter than the former, the distance d_n, in the case of $\mathcal{N}$ uniformly distributed particles, is:[70]

$$\frac{d_n}{L} = \frac{1}{\pi^{1/2}} \Big[\Gamma\Big(\frac{D}{2} + 1\Big) \Big]^{1/D} \frac{\Gamma(n + \frac{1}{D})}{\Gamma(n)} \Big(\frac{1}{\mathcal{N}}\Big)^{1/D}, \tag{A7}$$

with the mean square fluctuation,

$$\left(\frac{\Delta d_n}{L}\right)^2 = \frac{1}{\pi} \Big[\Gamma\Big(\frac{D}{2} + 1\Big) \Big]^{2/D} \left[\frac{\Gamma(n + \frac{2}{D})}{\Gamma(n)} - \frac{\Gamma^2(n + \frac{1}{D})}{\Gamma^2(n)} \right] \Big(\frac{1}{\mathcal{N}}\Big)^{2/D}. \tag{A8}$$

Results for the three test cases are presented in Figure 10, as a function of the neighbour index n. They show that, when $\mathcal{N} = 1000$, only the simulation with $L/L_0 = 8$ has average nth neighbour distance consistent, within error bars, with the theoretical prediction (Eqs. (A7) and (A8)). Thus,
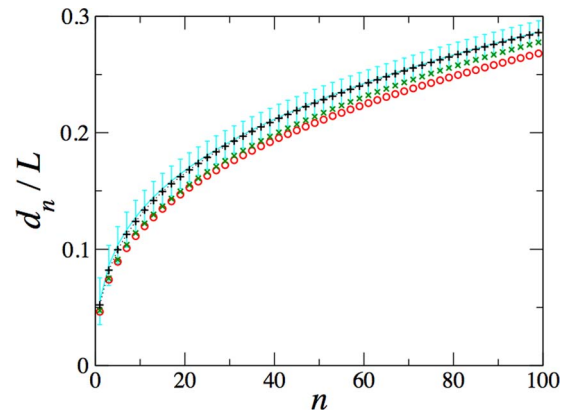
FIG. 10. Average nth neighbour distance for $n < 100$. The curves represent: the theoretical expectation with error bars (cyan), simulation with L/L_0 respectively equal to 8 (black pluses), 4 (green crosses), and 2 (red circles).

we infer that the ratio of correlated modes, N_c, to the total number of modes, N_m, has to be rather small in order for the model to satisfy incompressibility. The present indication is that $N_c/N_m \simeq 1/6$ is enough to produce uniformity at all scales (see Figure 9), with such a stringent test. When the present model is employed as a subgrid-scale Lagrangian model, this restriction can be relaxed as the evolution on the larger scales will be matched with the resolved modes of the LES.

[1] H. J. S. Fernando, D. Zajic, S. Di Sabatino, R. Dimitrova, B. Hedquist, and A. Dallman, "Flow, turbulence and pollutant dispersion in urban atmospheres," Phys. Fluids **22**, 051301 (2010).

[2] R. Scatamacchia, L. Biferale, and F. Toschi, "Extreme events in the dispersions of two neighboring particles under the influence of fluid turbulence," Phys. Rev. Lett. **109**, 144501 (2012).

[3] F. Toschi and E. Bodenschatz, "Lagrangian properties of particles in turbulence," Annu. Rev. Fluid Mech. **41**, 375 (2009).

[4] N. S. Holmes and L. Morawska, "Review of dispersion modelling and its application to the dispersion of particles: An overview of different dispersion models available," Atmos. Environ. **40**, 5902 (2006).

[5] M. Chamecki and C. Meneveau, "Particle boundary layer above and downstream of an area source: Scaling, simulations, and pollen transport," J. Fluid Mech. **683**, 1 (2011).

[6] G. Lacorata, A. Mazzino, and U. Rizza, "3D chaotic model for subgrid turbulent dispersion in large Eddy simulations," J. Atmos. Sci. **65**(7), 2389 (2008).

[7] A. S. Lanotte and I. M. Mazzitelli, "Scalar turbulence in convective boundary layers by changing the entrainment flux," J. Atmos. Sci. **70**, 248 (2013).

[8] S. Berti, F. A. Dos Santos, G. Lacorata, and A. Vulpiani, "Lagrangian drifter dispersion in the southwestern Atlantic ocean," J. Phys. Oceanogr. **41**, 1659 (2011).

[9] L. Palatella, F. Bignami, F. Falcini, G. Lacorata, A. S. Lanotte, and R. Santoleri, "Lagrangian simulations and inter-annual variability of anchovy egg and larva dispersal in the in the Sicily Channel," J. Geophys. Res.: Oceans **119**(2), 1306, doi:10.1002/2013JC009384 (2014).

[10] R. A. Shaw, "Particle-turbulence interactions in atmospheric clouds," Annu. Rev. Fluid Mech. **35**, 183 (2003).

[11] M. U. Baëbler, M. Morbidelli, and J. Badyga, "Modelling the breakup of solid aggregates in turbulent flows," J. Fluid Mech. **612**, 261 (2008).

[12] M. U. Baëbler, L. Biferale, and A. S. Lanotte, "Breakup of small aggregates driven by turbulent hydrodynamical stress," Phys. Rev. E **85**, 025301(R) (2012).

[13] S. Post and J. Abraham, "Modeling the outcome of drop-drop collisions in Diesel sprays," Int. J. Multiphase Flow **28**, 997 (2002).

[14] P. Segaut, *Large Eddy Simulation for Incompressible Flows*, 3rd ed. (Springer, 2006).

[15] C. Meneveau and J. Katz, "Scale-invariance and turbulence models for large-Eddy simulation," Annu. Rev. Fluid Mech. **32**(1), 1 (2000).

[16] P. P. Sullivan, J. C. McWilliams, and C.-H. Moeng, "A sub-grid-scale model for large-eddy simulation of planetary boundary layer flows," Bound.-Layer Meteorol. **71**, 247 (1994).

[17] E. Lévêque, F. Toschi, L. Shao, and J.-P. Bertoglio, "Shear-improved Smagorinsky model for large-eddy simulation of wall-bounded turbulent flows," J. Fluid Mech. **570**, 491 (2007).

[18] S. Ott and J. Mann, "An experimental investigation of the relative diffusion of particle pairs in three-dimensional turbulent flows," J. Fluid Mech. **422**, 207 (2000).

[19] A. La Porta, G. A. Voth, A. M. Crawford, J. Alexander, and E. Bodenschatz, "Fluid particle accelerations in fully developed turbulence," Nature (London) **409**, 1017 (2001).

[20] N. Mordant, P. Metz, O. Michel, and J. F. Pinton, "Measurement of Lagrangian velocity in fully developed turbulence," Phys. Rev. Lett. **87**, 214501 (2001).

[21] T. Ishihara and Y. Kaneda, "Relative diffusion of a pair of fluid particles in the inertial subrange of turbulence," Phys. Fluids **14**(11), L69 (2002).

[22] P. K. Yeung and M. S. Borgas, "Relative dispersion in isotropic turbulence: Part 1. Direct numerical simulations and Reynolds number dependence," J. Fluid Mech. **503**, 125 (2004).

[23] G. Boffetta and I. M. Sokolov, "Relative dispersion in fully developed turbulence: The Richardson's law and intermittency corrections," Phys. Rev. Lett. **88**, 094501 (2002).

[24] L. Biferale, G. Boffetta, A. Celani, B. J. Devenish, A. Lanotte, and F. Toschi, "Multifractal statistics of Lagrangian velocity and acceleration in turbulence," Phys. Rev. Lett. **93**, 064502 (2004).

[25] L. Biferale, G. Boffetta, A. Celani, B. J. Devenish, A. Lanotte, and F. Toschi, "Lagrangian statistics of particle pairs in homogeneous isotropic turbulence," Phys. Fluids **17**, 115101 (2005).

[26] P. K. Yeung, "Lagrangian investigations of turbulence," Annu. Rev. Fluid Mech. **34**, 115 (2002).

[27] B. Sawford, "Turbulent relative dispersion," Annu. Rev. Fluid Mech. **33**, 289 (2001).

[28] J. P. L. C. Salazar and L. R. Collins, "Two-particle dispersion in isotropic turbulent flows," Annu. Rev. Fluid Mech. **41**, 405 (2009).

[29] J. Bec, L. Biferale, A. S. Lanotte, A. Scagliarini, and F. Toschi, "Turbulent pair dispersion of inertial particles," J. Fluid Mech. **645**, 497 (2010).

[30] J. C. Weil, P. P. Sullivan, and C.-H. Moeng, "The use of large-Eddy simulations in Lagrangian particle dispersion models," J. Atmos. Sci. **61**, 2877 (2004).

[31] G. Jin and G.-W. He, "A nonlinear model for the subgrid timescale experienced by heavy particles in large eddy simulation of isotropic turbulence with a stochastic differential equation," New J. Phys. **15**, 035011 (2013).

[32] G. Falkovich, K. Gawędzki, and M. Vergassola, "Particles and fields in fluid turbulence," Rev. Mod. Phys. **73**, 913 (2001).

[33] M. Chertkov, A. Pumir, and B. Shraiman, "Lagrangian tetrad dynamics and the phenomenology of turbulence," Phys. Fluids **11**, 2394 (1999).

[34] L. Biferale, G. Boffetta, A. Celani, B. J. Devenish, A. Lanotte, and F. Toschi, "Multiparticle dispersion in fully developed turbulence," Phys. Fluids **17**, 111701 (2005).

[35] H. Xu, N. T. Ouellette, and E. Bodenschatz, "Evolution of geometric structures in intense turbulence," New J. Phys. **10**, 013012 (2008).

[36] J. F. Hackl, P. K. Yeung, and B. L. Sawford, "Multi-particle and tetrad statistics in numerical simulations of turbulent relative dispersion," Phys. Fluids **23**, 065103 (2011).

[37] A. Arnéodo *et al.*, "Universal intermittent properties of particle trajectories in highly turbulent flows," Phys. Rev. Lett. **100**, 254504 (2008).

[38] D. J. Thomson, "Criteria for the selection of stochastic models of particle trajectories in turbulent flows," J. Fluid Mech. **180**, 529 (1987).

[39] H. Kaplan and N. Dinar, "A three dimensional stochastic model for concentration fluctuation statistics in isotropic homogeneous turbulence," J. Comput. Phys. **79**, 317 (1988).

[40] D. J. Thomson, "A stochastic model for the motion of particle pairs in isotropic high-Reynolds number turbulence, and its application to the problem of concentration variance," J. Fluid Mech. **210**, 113 (1990).

[41] O. A. Kurbanmuradov, "Stochastic Lagrangian models for two-particle relative dispersion in high-Reynolds number turbulence," Monte Carlo Methods Appl. **3**, 37 (1997).

[42] B. J. Devenish and D. J. Thomson, "A Lagrangian stochastic model for tetrad dispersion," J. Turbul. **14**(3), 107 (2013).

[43] B. J. Devenish, "Geometrical properties of turbulent dispersion," Phys. Rev. Lett. **110**, 064504 (2013).

[44] J. C. H. Fung, J. C. R. Hunt, N. A. Malik, and R. J. Perkins, "Kinematic simulation of homogeneous turbulent flows generated by unsteady random Fourier modes," J. Fluid Mech. **236**, 281 (1992).

[45] J. C. H. Fung and J. C. Vassilicos, "Two-particle dispersion in turbulentlike flows," Phys. Rev. E **57**, 1677 (1998).

[46] M. Chaves, K. Gawędzki, P. Horvai, A. Kupiainen, and M. Vergassola, "Lagrangian dispersion in Gaussian self-similar velocity ensembles," J. Stat. Phys. **113**, 643 (2003).

[47] D. J. Thomson and B. J. Devenish, "Particle pair separation in kinematic simulations," J. Fluid Mech. **526**, 277 (2005).

[48] G. L. Eyink and D. Benveniste, "Suppression of particle dispersion by sweeping effects in synthetic turbulence," Phys. Rev. E **87**(2), 023011 (2013).

[49] J. G. M. Kuerten, "Subgrid modeling in particle-laden channel flow," Phys. Fluids **18**, 025108 (2006).

[50] C. Marchioli, M. V. Salvetti, and A. Soldati, "Some issues concerning large-Eddy simulation of inertial particle dispersion in turbulent bounded flows," Phys. Fluids **20**, 040603 (2008).

[51] E. Calzavarini, A. Donini, V. Lavezzo, C. Marchioli, E. Pitton, A. Soldati, and F. Toschi, "On the error estimate in sub-grid models for particles in turbulent flows," in *Direct and Large-Eddy Simulation VIII*, ERCOFTAC Series Vol. 15 (Springer, Netherlands, 2011), 171–176.

[52] J. J. Monaghan, "Smoothed particle hydrodynamics and its diverse applications," Annu. Rev. Fluid Mech. **44**, 323 (2012).

[53] B. L. Sawford, S. B. Pope, and P. K. Yeung, "Gaussian Lagrangian stochastic models for multi-particle dispersion," Phys. Fluids **25**, 055101 (2013).

[54] M. S. Borgas and B. L. Sawford, "A family of stochastic models for two-particle dispersion in isotropic homogeneous stationary turbulence," J. Fluid Mech. **279**, 69 (1994).

[55] T. Burgener, D. Kadau, and H. Herrmann, "Particle and particle pair dispersion in turbulence modeled with spatially and temporally correlated stochastic processes," Phys. Rev. E **86**, 046308 (2012).

[56] U. Frisch, *Turbulence: The legacy of A. N. Kolmogorov* (Cambridge University Press, New York, 1995).

[57] D. T. Gillespie, "Exact numerical simulation of the Ornstein-Uhlenbeck process and its integral," Phys. Rev. E **54**, 2084 (1996).

[58] S. B. Pope, *Turbulent Flows* (Cambridge University Press, 2000).

[59] C. Meneveau, "Transition between viscous and inertial-range scaling of turbulence structure functions," Phys. Rev. E **54**, 3657 (1996).

[60] V. Artale, G. Boffetta, A. Celani, M. Cencini, and A. Vulpiani, "Dispersion of passive tracers in closed basins: Beyond the diffusion coefficient," Phys. Fluids **9**, 3162 (1997).

[61] M. Cencini and A. Vulpiani, "Finite size Lyapunov exponent: Review on applications," J. Phys. A: Math. Theor. **46**, 254019 (2013).

[62] G. Boffetta and I. M. Sokolov, "Statistics of two-particle dispersion in two-dimensional turbulence," Phys. Fluids **14**, 3224 (2002).

[63] U. Frisch, A. Mazzino, and M. Vergassola, "Intermittency in passive scalar advection," Phys. Rev. Lett. **80**, 5532 (1998).

[64] A. Celani and M. Vergassola, "Statistical geometry in scalar turbulence," Phys. Rev. Lett. **86**(3), 424 (2001).

[65] A. Pumir, B. I. Shraiman, and M. Chertkov, "Geometry of Lagrangian dispersion in turbulence," Phys. Rev. Lett. **85**, 5324 (2000).

[66] G. Pagnini, "Lagrangian stochastic models for turbulent relative dispersion based on particle pair rotation," J. Fluid Mech. **616**, 357 (2008).

[67] L. Biferale, G. Boffetta, A. Celani, A. Crisanti, and A. Vulpiani, "Mimicking a turbulent signal: Sequential multiaffine processes," Phys. Rev. E **57**(6), R6261 (1998).

[68] M. R. Maxey and J. Riley, "Equation of motion of a small rigid sphere in a nonuniform flow," Phys. Fluids **26**, 883 (1983).

[69] S. Chandrasekhar, "Stochastic problems in physics and astronomy," Rev. Mod. Phys. **15**, 1 (1943).

[70] A. G. Percus and O. C. Martin, "Finite size and dimensional dependence in the Euclidean traveling salesman problem," Phys. Rev. Lett. **76**, 1188 (1996).